Brain Structure and Function
https://doi.org/10.1007/s00429-020-02079-6

ORIGINAL ARTICLE

The impact of phantom decoys on the neural processing of valuation

Shuyi Wu[1] · **Rongjun Yu**[2]

Received: 1 November 2019 / Accepted: 11 April 2020

Abstract
Rational decision theories posit that good choices should be based solely on information that is relevant to the choice at hand. However, introducing an inferior option that would never be chosen can influence choices among other relevant options, known as decoy effect. We used functional magnetic resonance imaging (fMRI) combined with a simple gambling task to investigate the neural signature of decision-making in or against the influence of the decoy effect in inferior and superior phantom decoy conditions. The fMRI results show that compared with choosing against the influence of the dominated phantom inferior option, choosing in the influence of the same option was associated with stronger activation in bilateral caudate and weaker functional connectivity between the left ventral anterior cingulate cortex (vACC) and the left caudate. Phantom inferior effect selectively enhanced the connectivity from the caudate to the vACC but not vice versa. Choosing in the influence of the dominated phantom superior option engaged greater activity in the left dorsal ACC and stronger functional connectivity between the left dACC and bilateral anterior insula. Furthermore, the direction of the phantom superior effect was restricted from left dACC to the anterior insula, but not vice versa. Our findings suggest that a phantom inferior decoy may boost the value of the target via the reward network, whereas a phantom superior decoy may diminish the value of the target option via the aversion network. Our study provides neural evidence to support that valuation is context dependent and delineates differential neural networks underlying the influence of unavailable inferior and superior decoy options on our decision-making.

Keywords Decoy effect · Phantom effect · Unavailable decoy · fMRI · DCM

Introduction

Rational decision theories posit that good choices should be based solely on information that is relevant to the choice at hand (Luce 2012). However, it is ubiquitously observed that preferences for two otherwise equally attractive options can change in the presence of a third option. For example, the choice between a powerful but more expensive laptop computer Y and a less powerful but more economical X can be systematically biased toward X by the presence of a third option Z that is less powerful but more expensive than X, which is known as decoy effect (Huber et al. 1982). If Z is more powerful and more economical than X but unavailable for buyers, the presence of Z can also bias individuals to choose Y, known as phantom decoy effect (Pratkanis and Farquhar 1992). Inferior decoys are less attractive in comparison with the target products and are rarely chosen. Phantom decoys, on the other hand, are attractive but unavailable alternatives: by definition, they are superior to the target products but not available, e.g. a superior product that is sold out (Pratkanis and Farquhar 1992).

Ample studies have demonstrated that decoy effects are quite robust in high-level decision tasks such as inference task (Trueblood 2012), performance ratings and evaluations (Ahn and Novoa 2016), risky choice tasks (Mohr et al. 2017; Tsetsos et al. 2012), intertemporal choice context (Gluth et al. 2017), and low-level perceptual choice task (Trueblood et al. 2013). Moreover, a few studies have

Electronic supplementary material The online version of this article (https://doi.org/10.1007/s00429-020-02079-6) contains supplementary material, which is available to authorized users.

✉ Rongjun Yu
psyyr@nus.edu.sg

[1] School of Psychology, Center for Studies of Psychological Application and Key Laboratory of Mental Health and Cognitive Science of Guangdong Province, South China Normal University, Guangzhou, People's Republic of China

[2] Department of Psychology, National University of Singapore, Block AS4, 02-17, 9 Arts Link, Singapore 117570, Singapore

Published online: 08 May 2020

found that individuals often show an increased preference for the option which is similar to the dominated but unavailable decoy (Ge et al. 2009; Pratkanis and Farquhar 1992). Some other researches have also found that when the phantom decoy is withheld (i.e. a brief delay but before a choice is made, or until after participants choose it), participants show preference for the competitor over the target both in consumer decision-making (Trueblood et al. 2013) as well as in perceptual decision choice (Trueblood and Pettibone 2017). These studies show that an option, even when it is not available, can still have an impact on decision-making.

Recent neuroscience research has found that choosing targets that are dominated by decoys rather than competitors that are not elicited stronger activity in the anterior insula (Hu and Yu 2014). Even when choosing a consistent option from a matching pair (the original two options are the same in both trials), choosing the option dominated by the decoy activated the ventral striatum, indicating that the presence of a decoy option influences the valuation of other options (Chung et al. 2017). Furthermore, some findings have revealed that the decoy effect was correlated with activities of brain areas implicated in cognitive control. For instance, activity in the anterior cingulate cortex (ACC) predicted a reduced susceptibility to the decoy effect (Hu and Yu 2014). Temporarily disrupting the right inferior frontal gyrus (rIFG), a region implicated in cognitive control, exhibited more context-dependent decision reversals (Chung et al. 2017). The dorsal ACC, along with anterior insula and superior parietal lobe, modulated decision control signals as predicted by the adaptive gain model in economic decoy dominating tasks (Li et al. 2018). A recent study found that transiently adding a low-value alternative, even when it was unavailable, led to a surprising failure of optimal decision-making, which was predicted by weaker value difference signals in the ventral medial prefrontal cortex (vmPFC) (Chau et al. 2014). Taken together, these studies suggest that the existence of decoys modulates the valuation system and choosing against the influence of the decoy effect recruits the cognitive control system.

Although the decoy effect is ubiquitous and theoretically important in challenging the belief that decision-making is context invariant, the neural basis of the effect remains largely underexplored, especially for phantom decoys, i.e. decoys that are not available. In the Chau et al. study, participants were shown the decoy options briefly for 100 ms and given 1.5 s to make a response. Given limited time for deliberation, participants may engage more satisficing strategies. Importantly, Chau et al. found that it was more difficult to choose the target when the distractor had a much lower value. However, surprisingly, in the Chau et al. study, when the unavailable decoy was more attractive than the target, participants still chose the target. It is still unclear whether inferior and superior phantom decoy share similar neural underpinnings. Moreover, compared to the perceptual domain, value-based decisions (also known as preferential choices) that employ complex choice options seem to have stronger context effects (Busemeyer et al. 2019; Farmer et al. 2017).

In the current study, we used fMRI combined with a gambling task to further investigate the neural signature of decision-making in or against the influence of the decoy in both inferior and superior phantom decoy conditions. According to the sequential sampling model, an attribute of the option that has an exceedingly high value should have a stronger influence on the decision. The recognition of such enhanced value was found to be encoded in the vmPFC (Hunt et al. 2014). We hypothesize that the overall subjective value of the target would be boosted by the lower valued attribute of the phantom inferior decoy, and that would be reflected as enhanced activity in reward-related regions such as caudate and ventral ACC. Accordingly, the overall subjective value of the target would be decreased by the higher valued attribute of the phantom superior decoy, and that might possibly be encoded in aversion-related brain areas such as dACC and insula. Functional connectivity analysis was conducted to delineate brain networks that contribute to the decoy effect in economic decision-making. We predicted that decision-making in the presence of phantom inferior decoy would be associated with signal flow changes among reward-related regions (from caudate to ventral ACC), whereas decision-making in the presence of phantom superior decoy would be related with functional connectivity changes among loss related regions (from dorsal ACC to insula).

Methods

Participants

Thirty-one healthy participants (mean age ± SD, 20.52 ± 1.77 years, 19 females) participated in return for payment. The sample size was determined based on the results of a previous fMRI study (Chung et al. 2017). All participants were right-handed and were screened for neurological or psychiatric disorders. The study was conducted with the approval of the local Institutional Review Boards. All participants gave written informed consent and were paid 60 yuan (~ 10 US dollars).

Experimental design and task procedure

Before the experiment, participants received instructions for the main task and were given 10 practice trials to ensure their understanding outside the scanner. In each trial, three gamble options appeared on the screen. The gamble options were presented for 4 s, after that a signal "×" was shown

below one of the options for 1 s, indicating that option was not available. Participants were instructed to make a choice within 4 s. No feedback was given to the participants (see Fig. 1a). The inter-trial interval is from 1 to 5 s. The gamble option was shown as a pie chart depicting the probability of winning a certain amount of money. The digit on the pie represents the result of the winning amount, and the size represents the probability of winning. The digits of the gamble options varied from ¥ 2 ($~0.32) to ¥ 96 ($~15.18) and the probabilities varied from 5 to 93%. The positions of options were counterbalanced. There were two types of phantom decoy conditions, that is phantom inferior decoy and phantom superior decoy, depending on whether the phantom decoy was superior or inferior to the target option. The phantom decoy option had either the same amount of money or the same probability, but with a lower/higher probability or amount of money than one of the two original gamble options, making this original gamble option the target, and the other original gamble option the competitor (see Table S1). In the control trials, the expected values of the three options were equivalent. We also included "catch" trials (one option was markedly better than others) to ensure that participants remained actively engaged.

For phantom inferior condition, in the matching pair of [A, B, A'], the phantom inferior A' is dominated by A (the target) but not by B (the competitor), whereas in [A, B, B'], the phantom inferior B' is dominated by B (the target) but not by A (the competitor). For phantom superior condition, in the matching pair of [A, B, A'], the phantom superior A' is dominated by B (the competitor) but not by A (the target). In [A, B, B'], the phantom superior B' is dominated by A (the competitor) but not by B (the target). The choice is said to be in the influence of the phantom inferior (Along PI) if the target is chosen (e.g., A is chosen from [A, B, A']) and against the influence of the phantom inferior (Against PI) if the competitor is chosen (e.g. A is chosen from [A, B, B']), see Fig. 1b. The choice is in the influence of the phantom superior (Along PS) when the competitor is chosen (e.g.

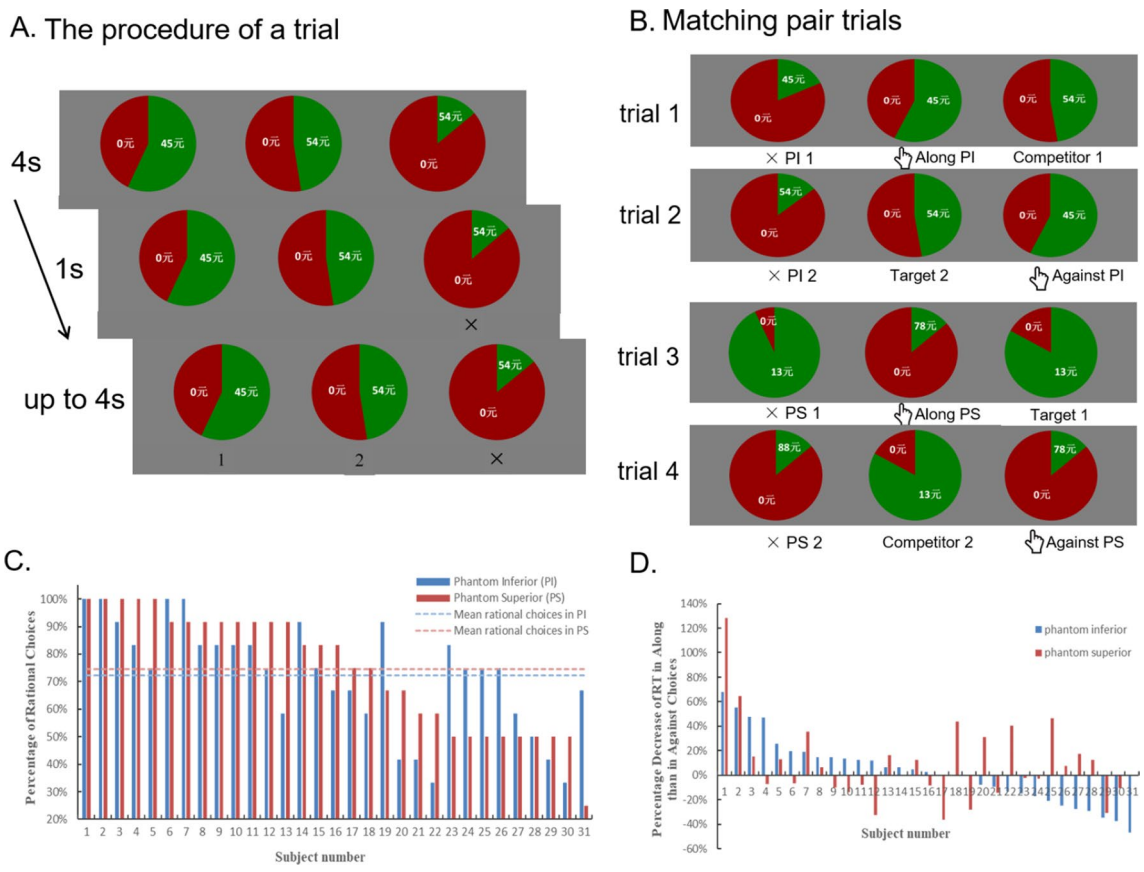

Fig. 1 **a** Experimental paradigm. Three gamble options were shown on the screen for 4 s. Then, a signal "×" below one of the option items for 1 s to indicate that this option was not available. After that, participants were instructed to make a choice between the two remaining options within 4 s. In the inferior/superior decoy condition, the unavailable option is similar to the target on one dimension and inferior/superior to the target on the other dimension. **b** Study design: matching pair of both phantom inferior trials and phantom superior trials. **c** Behavioural results. Percentages of rational choices in the phantom inferior and superior conditions for each participant are shown. **d** Behavioural results. Percentages decrease of RT in Along from Against choices

A is chosen from [A, B, B']) and against the influence of the phantom superior (Against PS) when the target is chosen (e.g., A is chosen from [A, B, A']), see Fig. 1b. The experiment had 96 trials (24 trials each condition) ordered randomly (Table S1). One trial was randomly chosen and implemented.

fMRI data acquisition and preprocessing

MRI scanning was conducted on a 3.0-T Siemens Trio scanner using a standard 12-channel head-coil system. Whole-brain data were acquired with echo planar T2*-weighted imaging (EPI), with the following parameters: 31 oblique axial slice, 3 mm thickness, 3 mm in-plane resolution; TR = 2000 ms; TE (echo time) = 30 ms; flip angle = 90°; FOV (field of view) = 224 mm; voxel size: 3 × 3 × 3 mm. T1-weighted structural images were acquired at a resolution of 1 × 1 × 1 mm.

fMRI data were analyzed using SPM12 (www.fil.ion.ucl.ac.uk/spm/). The first four images were discarded from the analysis for magnetization to reach a steady state. The EPI images were corrected for slice-timing differences and realigned to the first scan to correct for head movements. EPI and structural images were co-registered and normalized to the T1 standard template in Montreal Neurological Institute (MNI) space. Images were smoothed with a Gaussian kernel of full-width half-maximum 6 mm. Two subjects were excluded for having more than 2 mm of head motions.

fMRI data analysis

In general linear model 1 (GLM 1), we mainly included seven regressors of interest: choosing targets/competitors in or against the influence of the phantom inferior option in trials of matching pairs in phantom inferior condition, respectively (along PI/against PI); choosing competitors/targets in or against the influence of the phantom superior option in trials of matching pairs in phantom superior condition, respectively (along PS/against PS), control trials, catch trials and non-matching pairs (participants did not choose the same option in the matching pair trials). To identify brain regions encoding value difference between target and phantom decoy, we run GLM 2 with the following four regressors of interest: the expected value (EV) difference between target option and phantom inferior ($EV_{Target\text{-}PI}$), time locked to the onset of all phantom inferior trials, the EV difference between phantom superior and target option ($EV_{PS\text{-}Target}$), time locked to the onset of all phantom superior trials, control trials and catch trials. Six head-motion parameters calculated from the realignment were added to the GLM model as regressors of no interest. For the second-level analysis, a one-sample *t* test was performed to assess random effects at the group level.

To further investigate the signal change between target and phantom decoy, a finite impulse response (FIR) model was employed to extract the BOLD time courses across all voxels within regions of interest (ROIs) identified from GLM1 contrast analysis by MarsBaR 0.44 (https://marsbar.sourceforge.net/). Based on the group-level results, a 6-mm sphere ROI centred at the peak voxel was created in bilateral caudate and the left dACC (see "Results"). The time courses of trials associated with along/against phantom inferior and along/against phantom superior from all voxels within ROI were separately estimated across 24 time points from stimulus onset. Averaged parameter values of each time course across subject were displayed and SEs represented across-subject variability of the mean parameter estimates. To assess the statistical significance of beta values between two experimental conditions, we subjected each time point data to paired *t* test analysis.

Small volume correction (SVC) was used on prior regions of interest in reward and punishment processing: the caudate (Chung et al. 2017), the anterior cingulate cortex and the anterior insula (Hu and Yu 2014), defined by the corresponding automated anatomical labelling mask (Tzourio-Mazoyer et al. 2002). We reported regions that remained significant at a small-volume correction of FWE cluster-level threshold of $p < 0.05$. For the sake of completeness, we also reported brain regions across the whole brain that remained at $p < 0.001$ uncorrected, cluster voxels $k > 10$. For display purposes, all neural images are depicted at $p < 0.005$ uncorrected.

Psychophysiological interaction (PPI)

In addition to localize regional activity in response to experimental conditions, we also probed functional connectivity between brain areas to further understand the information flow between brain areas and changes in brain connectivity under different experimental contexts. PPI analysis was used to assess regionally specific functional connectivity that is modulated by psychological context (i.e. Along PI and Against PI in the present study) (Friston et al. 1997). The source regions were defined as 3 mm spheres centred at the peak voxel of the group-level conjunction results of two contrasts, including Along PI vs. Against PI in the phantom inferior condition and Along PS vs. Against PS in the phantom superior condition. The GLM for our PPI analysis was performed with three regressors: (1) the main effect of seed region activity, that is the physiological state, e.g. the time course of regional brain activity; (2) the main effect of phantom decoy effect, that is the psychological context; and (3) the interaction effect of seed region activity by the phantom decoy effect. The three regressors correspond to PPI.Y, PPI.P, and PPI.ppi in the GLM design matrix. Six head-motion parameters were also added to the model as

regressors of no interest. We sought to identify target regions for which the change in connectivity with the source region varied as a function of behavioural performance (i.e. phantom inferior effect, defined as the frequency of choosing targets' trials minus the frequency of choosing competitors' trials; phantom superior effect, defined as the frequency of choosing competitors' trials minus the frequency of choosing targets' trials). In the higher order PPI analysis, we included the behavioural effect size index as a covariate to investigate the relationship between behavioural phantom inferior/ phantom superior effect and functional connectivity in the brain.

Dynamic causal modelling (DCM) analysis

Our current results from higher level PPI analysis showed two distinct networks for different phantom decoy conditions. It is noteworthy that the anterior insula and dACC have been consistently found to be co-activated across a stream of tasks (Jung et al. 2014; Chang et al. 2013; Cauda et al. 2012; Li et al. 2018), such as the stop signal and go-no-go tasks (Swick et al. 2011). These regions were also found in the higher PPI results in the phantom inferior condition. However, few studies have investigated the signal flow within this network. It remains to be tested whether the direction of network connectivity between anterior insula and dACC could be causally mediated by the phantom superior effect. More interestingly, participants with lower phantom inferior effect at the behavioural level had stronger functional connectivity between the left caudate and left vACC (see "Result"). The anterior cingulate cortex has been shown to be recruited in executive control in value-based decision-making (Hu and Yu 2014; Gläscher et al. 2012). Here we address the issues of whether distinct ACC-related networks support different cognitive functions.

To achieve the goal mentioned above, we further conducted a dynamic causal modelling analysis to test directional information flow between the brain regions involved in phantom inferior and phantom superior conditions (Friston et al. 2003). DCM estimates three sets of parameters, including the intrinsic connections between regions independent of experimental context, the driving effect of external stimuli on specific regions, and the modulatory effect of stimuli on the effective connectivity between regions (Ewbank et al. 2011; Passamonti et al. 2008). Consistent with common approaches (Gandolla et al. 2014; Passamonti et al. 2008; Rothkirch et al. 2018), the nodes in our models were identified based on brain regions identified in our previous network connectivity analysis. In the phantom inferior condition, we create a 6-mm sphere ROI in the left caudate and the left vACC (see Tables 1 and 2). In the phantom superior condition, a 6-mm sphere ROI was created in the left dACC and the bilateral anterior insula (see Tables 1 and 2). The intrinsic connections (connectivity regardless the main effect of the task, DCM Bilinear matrix A value; see Fig. 3a) were modelled as bidirectional in accord with our group level analysis results. High-order PPI analysis results showing that the left caudate projects to the left vACC and vice versa in phantom inferior condition, whereas the left dACC projects to the bilateral anterior insula and vice versa in phantom superior condition. The modulation by either Along

Table 1 Brain regions activated at the stimuli phase

Contrast	Brain regions	z-score	Peak coordinate MNI (X, Y, Z)	Volume (voxel)
Along PI vs. against PI	Caudate**	3.26	− 12, − 3, 15	20
		3.26	12, − 3, 15	34
	Thalamus proper	3.89	− 3, − 9, 9	251
	Superior frontal gyrus	3.67	− 24, 39, 30	70
		3.33	18, 45, 36	59
	Occipital fusiform gyrus	3.47	− 27, − 69, − 15	213
	Precentral gyrus	3.00	48, − 6, 27	11
Against PI vs. along PI	No significant activation			
Along PS vs. against PS	Anterior cingulate gyrus	2.78	− 9, 39, − 6	115
	Anterior cingulate gyrus*	3.55	− 6, 27, 27	20
	Precentral gyrus	3.65	18, − 24, 72	165
	Superior frontal gyrus	2.99	− 9, 9, 66	11
Against PS vs. along PS	Inferior temporal gyrus	3.13	− 45, − 57, − 9	58
	Inferior occipital gyrus	3.12	− 45, − 66, − 6	58
	Fusiform gyrus	2.98	− 43, − 45, − 15	58

*$p < 0.05$ FWE after small volume correction, **indicates marginal significance (FWE) after small volume correction. The other regions remained at $p < 0.001$ uncorrected and a 10-voxel extent threshold. No brain region remained at cluster-level FWE $p < 0.05$ correction based on $p < 0.001$ uncorrected

Table 2 Parametric analysis results

Contrast	Brain regions	z-score	Peak coordinate MNI (X, Y, Z)	Volume (voxel)
Positive modulation with $EV_{Target\text{-}PI}$	vmPFC*	4.09	− 12, 42, − 6	38
		4.07	12, − 3, 15	34
	Ventral straitum*	5.13	− 12, 24, − 6	23
		4.81	12, 21, − 9	19
	Lingual gyrus[a]	5.42	6, − 90, − 6	708
	Superior temporal gyrus[a]	4.25	66, − 27, 6	209
	Middle frontal gyrus	4.08	− 36, 45, 33	57
	Central operculum	3.83	42, − 9, 12	26
	Supramarginal gyrus	3.75	− 57, − 45, 30	158
Negative modulation with $EV_{Target\text{-}PI}$	Fusiform gyrus[a]	3.85	− 33, − 48, − 21	77
		4.23	30, − 54, − 9	145
	Middle frontal gyrus	3.73	48, 45, 12	12
Positive modulation with $EV_{PS\text{-}Target}$	No significant activation			
Negative modulation with $EV_{PS\text{-}Target}$	Inferior frontal gyrus[a]	4.64	− 48, 6, 18	76
		5.47	48, 27, 27	373
	Fusiform gyrus[a]	6.61	− 45, − 60, − 15	4718
	Precentral gyrus[a]	4.21	− 30, − 12, 63	233
	Parahippocampal gyrus	3.92	− 30, − 24, − 27	13
	Posterior cingulate gyrus	3.37	6, − 36, 39	32
	Supramarginal gyrus	3.74	− 45, − 36, 45	78
	Middle frontal gyrus	3.41	− 42, 27, 30	14

*$p < 0.05$ FWE after small volume correction

[a]Brain region remained at cluster-level FWE $p < 0.05$ correction based on $p < 0.001$ uncorrected. The other regions remained at $p < 0.001$ uncorrected and a 10-voxel extent threshold

with phantom decoy or Against it was included as a bilinear effect expressing the contextual moderator (i.e. Along PI versus Against PI context in model 1; DCM Bilinear matrix B value, see Fig. 3a).

We tested six different DCM models (three models in each condition) in which the driving inputs (i.e. matching pair trials of PI/PS) were 'injected' into different parts of the network (Fig. 3). This 'injection' determines the origin of perturbation of the network, from which other points in the network will be activated according to the pattern of connectivity. In phantom inferior condition, for the first "parallel" models (model 1), matching pair trials of PI driving inputs (i.e. Along PI & Against PI) were 'injected' into both left caudate and the left vACC. The "serial" models differ from the first with respect to where the driving inputs were injected: only in the left caudate (model 2) or only in the left vACC (model 3, Fig. 3a). In phantom superior condition, for the first "parallel" models (model 1), matching pair trials of PS driving inputs (i.e. Along PS & Against PS) were 'injected' into both left dACC and the bilateral anterior insula. In the "serial" models, the driving inputs were injected only in the left dACC (model 2) or only in the bilateral anterior insula (model 3, Fig. 3b).

The Bayesian model selection (BMS) procedure was used to determine the best model, which is based on comparing the model evidence of predefined models. The model evidence is the probability of generating the observed data by a specific model (Penny et al. 2004). We applied a random-effects BMS approach to infer the optimal model structure by selecting the model with the best balance between accuracy and complexity (Stephan et al. 2009). A common measure for the group evidence of a given model is to report the exceedance probability (EP), i.e. the extent to which each model is more likely than any other model to have generated the data from a randomly selected participant (Ewbank et al. 2011). Following the model selection, we performed a random-effects analysis of parameter estimates derived from the selected model using one-sample *t* tests.

Results

Behaviour results

The percentage of choosing the gamble options which had markedly higher expected outcomes was 95.4% ± 4.2%

(mean ± SD) in "catch" trials. Participants were highly accurate in making correct choices in these "catch" trials, providing evidence of continued engagement with the task throughout the experiment.

In the "control" trials, the expected values of three options were equivalent. The percentage of choosing the far left option is significantly larger than the middle option ($M_{diff} = 0.07$, SE = 0.02, $p < 0.01$) and the far right one ($M_{diff} = 0.08$, SE = 0.02, $p < 0.01$), whereas no significant difference between the middle and the far right option ($M_{diff} = 0.005$, SE = 0.02, $p > 0.1$).

Generally, rational choices (also known as context-independent behaviours) would choose the consistent choices from the matching trials: the subject chose the same option A in both [A, B, A'] and [A, B, B'] trials, while the non-rational choices (also known as context-dependent effect) would favour targets: the subject chose the target in both trials (i.e. switched from A to B when the inferior decoy changed from A' to B'). In the phantom inferior condition, 72.31% of the matching pairs were behaviourally rational and 25.00% were non-rational. In the phantom superior condition, 74.46% of the matching pairs were behaviourally rational and 22.04% were non-rational, see Fig. 1c. Phantom decoy effects that come from the proportions of choosing targets compared with the proportions of choosing competitors were not significantly different, typically occurring about 20% of the frequency in non-rational choices, which are in line with previous studies (Chung et al. 2017; Hu and Yu 2014).

Because the great majority of matching pairs were behaviourally rational, choices in this experiment were largely context independent. However, the valuations of target options might still be influenced by decoys, even though such context-dependent valuation is not powerful enough to elicit changes in choices. Thus, we compare the 'Along' trials with the 'Against' trials of the matching pair as the previous research did (Chung et al. 2017). Across all subjects, the average reaction times (RT) of rational trials which are Along PI and Against PI were 840 ms and 847 ms, respectively. In comparison, the average RT of rational trials which are Along PS and Against PS were 931 ms and 871 ms, respectively. Of all Along PI trials, the average percentage decrease in RT is 3%. But for rational trials, the percentage decrease in RT of Along PI from Against PI trials is not significantly different from zero, p(one tail) = 0.286. On the other hand, while the average percentage decrease in RT of all Along PS trials is 9%, in rational trials, the percentage decrease in RT of Along PS from Against PS trials is marginally significant, p(one-tail) = 0.067, see Fig. 1d.

fMRI results

The phantom inferior effect was defined by choosing targets in the direction of the influence of the phantom inferior decoy (Along PI) versus choosing competitors against the phantom inferior (Against PI) contrast. The phantom superior effect was defined by choosing competitors in the direction of the influence of the phantom superior decoy (Along PS) versus choosing targets against the phantom superior (Against PS) contrast (see Fig. 1). All the significantly activated brain areas related to the experimental factors are shown in Table 1. Parametric analyses of neural activation (GLM 2) showed activities in distinct brain regions that were modulated by the relative expected value between the phantom decoy and target option (see Table 2). We further used PPI to examine the task-dependent functional connectivity of the phantom decoy effect. Using left caudate/left dACC as ROI seeds, we conducted PPI analyses in the Along PI/PS vs. Against PI/PS contrast of phantom inferior and phantom superior conditions, respectively (results are shown in Table 3).

We aim to unveil the neural mechanisms underlying the phantom inferior and phantom superior effects. If valuations are independent of the context, then after controlling for the same expected value of both the target and the competitor in each matching rational trial, the brain area processing valuation should not differentiate between Along PI/PS and Against PI/PS trials. In other words, if valuations are based on the context, then targets dominated by the phantom inferior or the phantom superior might be valued higher or lower than competitors. Hence, the activation of reward or loss-valuation areas are predicted to be stronger in trials that go with the influence (Along) rather than against the influence (Against) of decoys. Our fMRI data supported this prediction.

In the phantom inferior condition, we observed that choosing in the influence of the dominated decoy activated bilateral caudate (left: − 12, − 3, 15; peak z = 3.26, p(FWE) = 0.051 svc; right: 12, − 3, 15, peak z = 3.26, p(FWE) = 0.052 svc, see Fig. 2a). In contrast, when choosing against the influence of the dominated decoy, no significant activation was found in the brain regions of interest. Time courses revealed significantly higher parameter estimate from Along phantom inferior trials than Against phantom inferior contrast within the left caudate ROI by 6 s and 8 s post-stimulus onset, $t(28) = 2.699$, $p < 0.01$, $t(28) = 1.728$, $p < 0.05$; also within the right caudate ROI by 6 s post-stimulus onset, $t(28) = 3.181$, $p < 0.005$, see Fig. 2a. For the positive correlation of parametric modulation by $EV_{(Target-PI)}$, we found significant activations in the bilateral vmPFC (left: − 12, 42, − 6, peak z = 4.09, p(FWE) = 0.006 svc; right: 9, 42, − 15, peak z = 4.15, p(FWE) = 0.023 svc) and bilateral ventral striatum (left: − 12, 24, − 6, peak z = 5.13,

Table 3 Functional connectivity of the different contrasts in both phantom inferior and superior decoy as a function of behavioural phantom decoy effect

Contrast	Seed	Brain regions	z-score	Peak coordinate MNI (X, Y, Z)	Volume (voxel)
Along PI vs. against PI	L Caudate (− 12, − 3, 15)	Anterior cingulate gyrus*	4.22	− 3, 39, 12	41
		Anterior cingulate gyrus	4.22	− 3, 39, 12	71
	R Caudate (12, − 3, 15)	Middle temporal gyrus	3.45	− 54, 21, 6	158
		Angular gyrus	2.81	51, − 66, 36	10
Along with PS vs. against PS	L ACC (− 6, 27, 27)	Anterior insula*	4.07	− 33, 0, 12	95
			4.34	39, 3, 15	56
		Calcarine cortex	4.49	− 18, − 69, 6	1831
		Thalamus proper	4.48	− 6, − 3, 6	1831
		Central operculum	4.34	39, 3, 15	287
		Inferior frontal gyrus	3.54	51, 18, 27	287
		Middle frontal gyrus	4.23	42, 54, 12	163
			3.28	− 42, 51, 18	133
		Supramarginal gyrus	3.73	− 54, − 51, 24	66
		Supplementary motor cortex	3.63	6, 12, 66	122
		Precentral gyrus	3.50	54, − 3, 24	49
			3.11	− 24, − 24, 63	17
		Pallidum	3.42	21, − 6, − 3	24
		Caudate	3.25	18, 6, 21	31
		Anterior cingulate gyrus	3.13	− 6, 27, 30	16

The functional connectivity analysis was conducted using a PPI between Along PI and Against PI/Along PS and Against PS conditions with the bilateral caudate/left ACC as seeds. Phantom inferior effect at the behavioural level was defined by "choosing targets trials—choosing competitors trials"/all trials, whereas the phantom superior effect was defined by "choosing competitors—choosing targets trials"/all trials

*$p < 0.05$ FWE after small volume correction. The other regions remained at $p < 0.001$ uncorrected and a 10-voxel extent threshold. L: left; R: right

p(FWE) = 0.009 svc; right: 12, 21, − 9, peak z = 4.81, p(FWE) = 0.012 svc, Fig. 2c). No activations in the region of interest showed a negative correlation with parametrically modulated $EV_{(Target\text{-}PI)}$ regressor. These results showed that the larger the relative $EV_{(Target\text{-}PI)}$, the stronger the activation in reward-related brain regions, including vmPFC and bilateral caudate. The high-order PPI results showed that participants who were less susceptible to the phantom inferior effect at the behavioural level had stronger functional connectivity between the left caudate and left vACC (− 3, 39, 12, peak z = 4.22, p(FWE) = 0.003 svc, Fig. 2e). Participants who were more susceptible to the phantom inferior effect showed less activation in the vACC (Fig. 2f). In other words, subjects who were less susceptible to the phantom inferior effect had higher levels of coupling between the left caudate and left vACC when choosing targets compared to competitors of matching pairs in the phantom inferior condition.

In the phantom superior condition, we found that choosing along the dominated decoy relative to choosing against the dominated phantom superior activated left dACC (− 6, 27, 27; peak z = 4.03, p(FWE) = 0.033 svc, see Fig. 2b). No significant activation in the brain regions of interest was found for the reverse contrast. Time courses elicited significantly higher parameter estimate from Along phantom superior trials than Against phantom superior contrast within the left dACC ROI by 6 s, 8 s and 20 s following the stimulus onset, $t(28) = 2.009$, $p < 0.05$, $t(28) = 2.712$, $p < 0.01$, $t(28) = 1.903$, $p < 0.05$, and also marginal significantly higher parameter estimate from the contrast within the ROI by 22 s following the stimulus onset, $t(28) = 1.616$, $p = 0.059$, see Fig. 2b. The parametric analysis revealed that bilateral IFG (left: − 48, 6, 18; peak z = 4.64, p(FWE) = 0.002 svc; right: 48, 27, 27, peak z = 5.47, p(FWE) = 0.000), was negative modulated by the $EV_{(Target\text{-}PS)}$; see Fig. 2d. No activations showed a positive correlation with parametrically modulated $EV_{(Target\text{-}PS)}$ regressor. These results showed that the smaller the relative EV, the stronger the activation in cognitive control-related brain regions, including bilateral IFG. In the high-order PPI analysis, we found that participants who are more susceptible to the phantom superior effect at the behavioural level had stronger functional connectivity between the left dACC and the bilateral anterior insula (left: − 33, 0, 12, peak z = 4.84, p(FWE) = 0.003 svc; right: 39, 3, 15, peak z = 4.34, p(FWE) = 0.001 svc, Fig. 2g). They also showed a stronger activation in the bilateral anterior insula (Fig. 2h). In other words, subjects who were susceptible

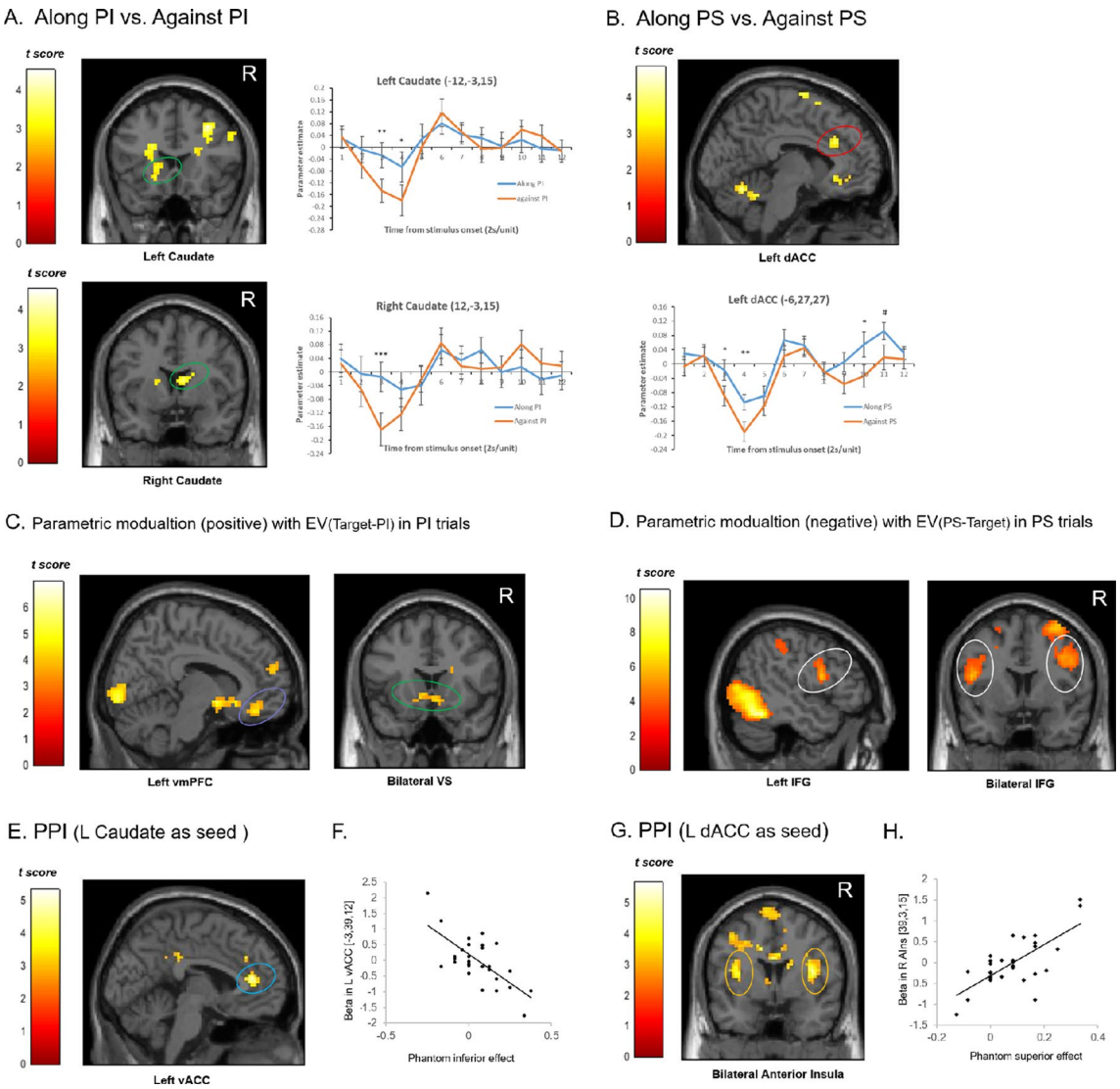

Fig. 2 fMRI results. **a** Left, bilateral caudate (x = ± 12, y = − 3, z = 15) was significantly activated by Along PI vs. Against PI contrast. Right, parameter estimates averaged across all voxels within bilateral caudate are shown from stimulus onset. Asterisks indicate time points at which value from along phantom inferior and against phantom inferior trials differed: $^{***}p < 0.001$, $^{**}p < 0.01$ and $^{*}p < 0.05$. **b** Left, the left ACC (x = − 6, y = 27, z = 27) was significantly activated by Along PS vs. Against PS. Right, parameter estimates averaged across all voxels within left dACC are shown from stimulus onset. Asterisks indicate time points at which value from two conditions differed: $^{**}p < 0.005$, $^{*}p < 0.05$ and $^{\#}p = 0.0587$. **c** Bilateral ventral striatum (VS) and bilateral vmPFC were activated by modulation with value difference between the target option and the phantom inferior option (i.e., $EV_{target\text{-}PI}$). **d** Bilateral IFG correlated parametrically with the value difference between the phantom superior and the decoy option (i.e., $EV_{PS\text{-}Target}$). **e** Participants with a smaller phantom inferior effect at the behavioural level showed stronger functional connectivity between the left caudate and left ACC in the phantom inferior condition. **f** The correlation between phantom inferior effect and parameter estimates of left vACC activation for Along PI vs. Against PI contrast at a peak voxel (− 3, 39, 12). **g** Participants with a larger phantom effect at the behavioural level showed stronger functional connectivity between the left ACC and anterior insula in the phantom superior condition. **h** The correlation between phantom superior effect and parameter estimates of right anterior insula activation for Along PS vs. Against PS contrast at a peak voxel (39, 3, 15). Along PI: choosing targets in the influence of the phantom decoy of trials in matching pairs in phantom inferior condition; Against PI: choosing competitors against the influence of the phantom decoy of trials in matching pairs in the phantom inferior condition; Along PS: choosing competitors in the influence of the phantom decoy of trials in matching pairs in phantom superior condition; Against PS: choosing targets against the influence of the phantom decoy of trials in matching pairs in phantom superior condition

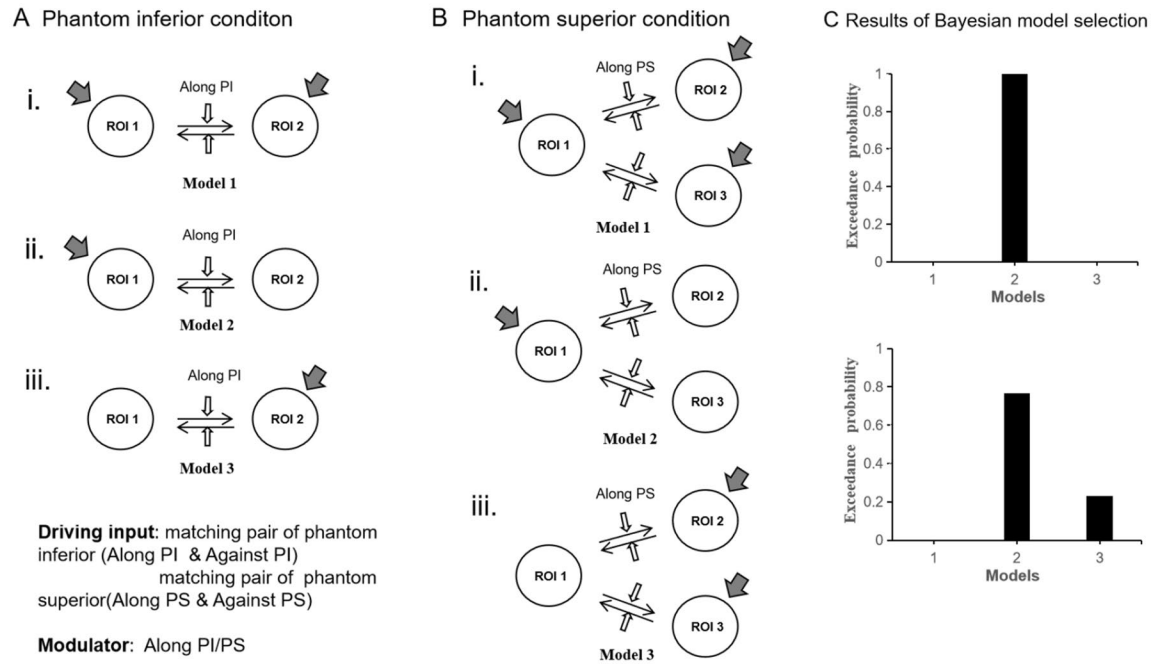

Fig. 3 Dynamic causal modelling (DCM) neural network. **a** In phantom inferior condition, the left caudate (ROI 1) and the left ACC (ROI 2) are the regions of interest according to the results of previous group-level analysis and high-order PPI analysis. The matching-pair trials of phantom inferior were entered as driving input (DCM matrix C values) directly in ROI 1 or ROI 2 or both the ROIs. The intrinsic connectivity between ROIs (DCM matrix A values) was modelled as bidirectional (see "DCM methods" for further details). Along PI was used as the bilinear modulator (DCM matrix B values) of connectivity in both pathways (from left caudate to left ACC and from left ACC to left caudate). **b** In phantom superior condition, the left ACC (ROI 1), the left anterior insula (ROI 2) and the right ACC (ROI 3) are the regions of interest according to the results of previous group-level analysis and high-order PPI analysis. The matching pair of phantom superiors were entered as driving input (DCM matrix C values) directly in ROI 1 or ROI 2 and 3 or both the ROIs. The intrinsic connectivity between ROIs (DCM matrix A values) was modelled as bidirectional. Along PS was used as the bilinear modulator (DCM matrix B values) of connectivity in both pathways (from left ACC to bilateral anterior insula and from bilateral anterior insula to left ACC). **c** Comparison between the three models divided from each condition using Bayesian model selection showed in the A and B. The model 2 outperformed all other models with the highest exceedance probability both in phantom inferior (upper panel) and phantom superior condition (lower panel)

to phantom superior effect had stronger levels of coupling between the left dACC and anterior insula when choosing targets compared to competitors of matching pairs in the phantom superior condition.

DCM results

Results of BMS showed that model 2 was associated with the highest exceedance probability of 100% in phantom inferior condition and 77% in phantom superior condition to explain the data (Fig. 3c). Therefore, we used model 2 to test the modulatory influence of Along PI (vs. Against PI) on each specific pathway (from left caudate to left ACC and from left ACC to left caudate), and to test the modulatory influence of Along PS (vs. Against PS) on each specific pathway (from left ACC to bilateral anterior insula and from bilateral anterior insula to left ACC).

As predicted, for phantom inferior condition, the intrinsic connectivity (DCM matrix A) between the ROIs in the whole sample was highly significant in both directions (from left caudate to left vACC and vice versa, $p < 0.001$, Fig. 4). The main effect of phantom inferior effect (Along PI versus Against PI context, DCM Bilinear matrix B) enhanced the connectivity from left caudate to left vACC ($p < 0.01$) but not vice versa ($p > 0.1$) across individuals (one-sample t test) (Fig. 4a). Choosing competitors against the phantom inferior in the matching pair trials (Against PI, DCM matrix C) had a very strong influence on the neural activity of left caudate ROI1 in all participants ($p < 0.01$) rather than choosing targets ($p > 0.1$, Fig. 4a).

For phantom superior condition, the intrinsic connectivity (DCM matrix A) between the ROIs in the whole sample was highly significant in both directions (from the left dACC to bilateral anterior insula and vice versa in phantom superior condition) ($p < 0.001$, Fig. 4). The main effect of phantom superior effect (Along PS versus Against PS context, DCM Bilinear matrix B) enhanced the connectivity from left dACC to bilateral anterior insula ($p < 0.05$) but not vice versa ($p > 0.1$) across individuals (one-sample t test) (Fig. 4b). Choosing targets along the phantom superior in

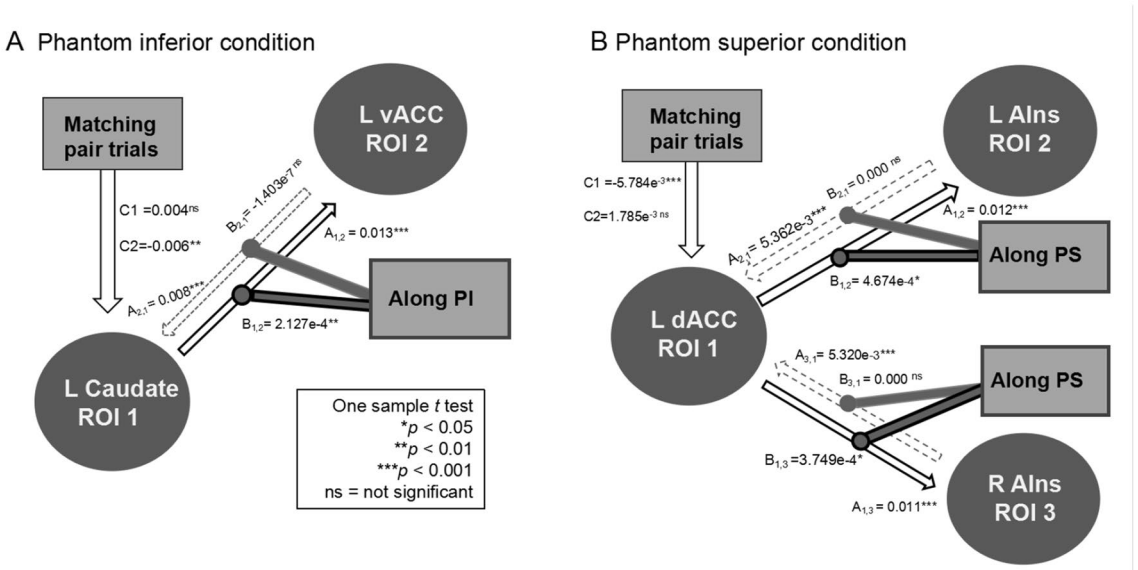

Fig. 4 Summary of the DCM results of preferred models from the whole group. The picture shows the DCM matrix mean values (A, B, and C) obtained from 29 participants (one-sample *t* test). **a** In phantom inferior condition, choosing competitors against the influence of the phantom inferior decoy in matching-pair trials (DCM matrix C2 values) have a very strong impact on the activity of the left caudate (ROI 1). The intrinsic connectivity (DCM matrix A values—regardless of experimental manipulation) was highly significant in both directions. In contrast, phantom inferior effect (DCM bilinear matrix B) selectively enhanced the connectivity from left caudate to left vACC ($B_{1,2}$) but not vice versa ($B_{2,1}$). **b** In phantom superior condition, choosing competitors in the influence of the phantom superior decoy in matching-pair trials (DCM matrix C1 values) have a very strong impact on the activity of the left dACC (ROI 1). The intrinsic connectivity (DCM matrix A values—regardless of experimental manipulation) was highly significant in both directions. In contrast, phantom superior effect (DCM bilinear matrix B) selectively enhanced the connectivity from left dACC to bilateral anterior insula ($B_{1,2}$; $B_{1,3}$), but not vice versa ($B_{2,1}$; $B_{3,1}$). *DCM* dynamic causal modelling. *ROI* region of interest

the matching pair trials (Along PS, DCM matrix C) had a very strong influence on the neural activity of left dACC ROI1 in all participants ($p < 0.01$) rather than choosing competitors ($p > 0.1$, Fig. 4b).

Discussion

In the current study, our fMRI results showed that the activation of the bilateral caudate increased in Along PI versus Against PI trials. In the phantom superior condition, choosing in the influence of the decoy effect engaged greater activity in the left dACC. Furthermore, high-order PPI results showed that behavioural phantom inferior effect was negatively correlated with connectivity between the left vACC and the left caudate. The behavioural phantom superior effect was positively correlated with connectivity between the left dACC and the bilateral anterior insula. Specifically, results of DCM showed that phantom inferior effect enhanced the connectivity from the left caudate to the left vACC, but weakened the connectivity from the left vACC to the left caudate, whereas phantom superior effect selectively enhanced the connectivity from the left dACC to bilateral anterior insula but not vice versa.

Despite widespread interests in the psychological mechanisms of decoy effect, the neural processes underlying decoy effects remain unclear. Using a biophysical model of multiple option decision-making, Chau et al. found that value difference (target minus competitor) signals in the vmPFC were decreased in the presence of low-value decoys, suggesting that a poor alternative modulates value difference signals. Furthermore, Chung et al. found that left ventral striatum was more active when the chosen option was dominated by the decoy, indicating that choosing in the influence of the decoy effect is rewarding. Importantly, it was found that right inferior frontal gyrus connected more strongly with the striatum when subjects successfully overrode the decoy effect and made unbiased choices (Chung et al. 2017), suggesting that the control system modulates the context-dependent activation of the valuation area. Taken together, these previous studies suggested that the reward valuation network is involved in assessing the decoy effect.

In our study, in the phantom inferior condition, consistent with recent work showing that left ventral striatum was more active when the chosen option dominated the decoy (Chung et al. 2017), a contrast of Along PI trials versus Against PI trials elicited stronger activation in the left caudate. Prior studies have shown that caudate encodes reward values

(Balleine et al. 2007; Kirschner et al. 2016). This finding may suggest that the same chosen option seems to be more valuable when it is the target than when it is not boosted by the decoy. Moreover, using the value difference between target option and phantom inferior option as a parametric modulator, we found that the larger the value difference, the stronger the activity in the reward regions, i.e. vmPFC and ventral striatum. This finding further corroborates the idea that the mere presence of an inferior decoy enhances the value of the target option. We also found that participant who has weaker context-dependent bias exhibits stronger functional connectivity between the left vACC and the left caudate. This finding indicates that the changes in coupling between two regions in response to the phantom inferior effect (Along PI) explained the individual behavioural differences in sensitivity to phantom inferior decoys. The dynamic causal modelling results revealed that phantom inferior effect selectively enhanced the neural connectivity from the caudate to vACC. These findings suggest an intriguing pattern that choosing in the influence of the phantom inferior decoy is perceived as more rewarding.

In the phantom superior condition, we found that choosing in the influence of the phantom superior decoy activated the dACC. The dACC has been involved in processing negative outcomes, such as performance errors and monetary losses (Yu and Zhou 2009; Woo et al. 2014). One possibility is that adding phantom superior options decreased the value of target options. This disposition is further supported by the parametric analysis showing that the value difference between the phantom superior option and the target option strongly modulated activity in the IFG. That is, when the value of the phantom superior option and the value of the target option are closer to each other, the IFG is more strongly activated. The IFG has been proposed to be involved in modulating the competitive weights of different stimulus response mappings to facilitate optimal decisions (Hampshire et al. 2010; Yaple and Yu 2019). Our findings suggest an important role of the IFG in processing choice conflict. Higher order PPI results revealed that bilateral anterior insula exhibits stronger functional connectivity with the left dACC in individuals who showed stronger phantom superior effect. Further, DCM analysis revealed that phantom superior effect selectively enhanced the connectivity from dACC to bilateral anterior insula. This finding is consistent with the majority of researches linking decoy effect to the anterior insula (Hedgcock and Rao 2009; Mohr et al. 2017). The anterior insula may also reflect greater salience detection and processing associated with choosing the dominated targets rather than competitors (Hu and Yu 2014).

Consistent with the recent fMRI study (Chung et al. 2017), we did not find significant decoy effects at the behavioural level. Even though decision-making was largely context independent, we found evidence that valuation of the target options at the neural level can be influenced by phantom decoys. To find out how (or when) valuation at the neural level can directly constrain cognitive choices, future research should focus more on applying computational models of the decoy effect to both brain and behavioural data (Busemeyer et al. 2019; Turner et al. 2017).

In conclusion, our research further documents the neural signature of the asymmetrically dominated phantom decoy. Choosing in the influence of the phantom inferior effect and phantom superior effect engaged the caudate-vACC and dACC-insula, respectively. Inconsistent with the independence of irrelevant alternatives (IIA) axiom, our study provides neural evidence supporting the context-dependent valuation. Our findings suggest that a phantom inferior decoy may boost the value of the target via the reward network, whereas a phantom superior decoy may diminish the value of the target option via the aversion network.

Compliance with ethical standards

Conflict of interest The authors have no conflicts of interest to declare.

Ethical approval The study was approved by the Institutional Ethical Review Board, in accordance with the declaration of Helsinki.

Informed consent All participants gave written informed consent.

References

Ahn H, Novoa NV (2016) The decoy effect in relative performance evaluation and the debiasing role of DEA. Eur J Oper Res 249(3):959–967

Balleine BW, Delgado MR, Hikosaka O (2007) The role of the dorsal striatum in reward and decision-making. J Neurosci 27(31):8161–8165

Busemeyer JR, Gluth S, Rieskamp J, Turner BM (2019) Cognitive and neural bases of multi-attribute, multi-alternative, value-based decisions. Trends Cogn Sci 23(3):251–263

Cauda F, Costa T, Torta DM, Sacco K, D'Agata F, Duca S, Geminiani G, Fox PT, Vercelli A (2012) Meta-analytic clustering of the insular cortex: characterizing the meta-analytic connectivity of the insula when involved in active tasks. Neuroimage 62(1):343–355

Chang LJ, Yarkoni T, Khaw MW, Sanfey AG (2013) Decoding the role of the insula in human cognition: functional parcellation and large-scale reverse inference. Cereb Cortex 23(3):739–749

Chau BK, Kolling N, Hunt LT, Walton ME, Rushworth MF (2014) A neural mechanism underlying failure of optimal choice with multiple alternatives. Nat Neurosci 17(3):463

Chung HK, Sjöström T, Lee HJ, Lu YT, Tsuo FY, Chen TS, Chang CF, Juan CH, Kuo WJ, Huang CY (2017) Why Do Irrelevant Alternatives Matter? An fMRI-TMS Study of Context-Dependent Preferences. J Neurosci 37(48):11647

Ewbank MP, Lawson RP, Henson RN, Rowe JB, Passamonti L, Calder AJ (2011) Changes in "top-down" connectivity underlie repetition suppression in the ventral visual pathway. J Neurosci 31(15):5635–5642

Farmer GD, Warren PA, El-Deredy W, Howes A (2017) The effect of expected value on attraction effect preference reversals. J Behav Decis Mak 30(4):785–793
Friston KJ, Buechel C, Fink GR, Morris J, Rolls E, Dolan RJ (1997) Psychophysiological and modulatory interactions in neuroimaging. Neuroimage 6(3):218–229
Friston KJ, Harrison L, Penny W (2003) Dynamic causal modelling. Neuroimage 19(4):1273–1302
Gandolla M, Ferrante S, Molteni F, Guanziroli E, Frattini T, Martegani A, Ferrigno G, Friston K, Pedrocchi A, Ward NS (2014) Re-thinking the role of motor cortex: context-sensitive motor outputs? Neuroimage 91(100):366–374
Ge X, Messinger PR, Li J (2009) Influence of soldout products on consumer choice. J Retail 85(3):274–287
Gläscher J, Adolphs R, Damasio H, Bechara A, Rudrauf D, Calamia M, Paul LK, Tranel D (2012) Lesion mapping of cognitive control and value-based decision making in the prefrontal cortex. Proc Natl Acad Sci 109(36):14681–14686
Gluth S, Hotaling JM, Rieskamp J (2017) The attraction effect modulates reward prediction errors and intertemporal choices. J Neurosci 37(2):371–382
Hampshire A, Chamberlain SR, Monti MM, Duncan J, Owen AM (2010) The role of the right inferior frontal gyrus: inhibition and attentional control. Neuroimage 50(3):1313–1319. https://doi.org/10.1016/j.neuroimage.2009.12.109
Hedgcock W, Rao AR (2009) Trade-off aversion as an explanation for the attraction effect: a functional magnetic resonance imaging study. J Mark Res 46(1):1–13
Hu J, Yu R (2014) The neural correlates of the decoy effect in decisions. Front Behav Neurosci 8:271
Huber J, Payne JW, Puto C (1982) Adding asymmetrically dominated alternatives: violations of regularity and the similarity hypothesis. J Consum Res 9(1):90–98
Hunt LT, Dolan RJ, Behrens TE (2014) Hierarchical competitions subserving multi-attribute choice. Nat Neurosci 17(11):1613
Jung Y-C, Schulte T, Müller-Oehring EM, Hawkes W, Namkoong K, Pfefferbaum A, Sullivan EV (2014) Synchrony of anterior cingulate cortex and insular-striatal activation predicts ambiguity aversion in individuals with low impulsivity. Cereb Cortex 24(5):1397–1408
Kirschner M, Hager OM, Bischof M, Hartmann-Riemer MN, Kluge A, Seifritz E, Tobler PN, Kaiser S (2016) Deficits in context-dependent adaptive coding of reward in schizophrenia. NPJ schizophrenia 2:16020
Li V, Michael E, Balaguer J, Castañón SH, Summerfield C (2018) Gain control explains the effect of distraction in human perceptual, cognitive, and economic decision making. Proc Natl Acad Sci 115(38):E8825–E8834
Luce RD (2012) Individual choice behavior: a theoretical analysis. Dover Publications, Mineola, NY (Original work published 1959)
Mohr PN, Heekeren HR, Rieskamp J (2017) attraction effect in risky choice can be explained by subjective distance between choice alternatives. Sci Rep 7(1):8942
Passamonti L, Rowe JB, Ewbank M, Hampshire A, Keane J, Calder AJ (2008) Connectivity from the ventral anterior cingulate to the amygdala is modulated by appetitive motivation in response to facial signals of aggression. Neuroimage 43(3):562–570
Penny WD, Stephan KE, Mechelli A, Friston KJ (2004) Comparing dynamic causal models. Neuroimage 22(3):1157–1172
Pratkanis AR, Farquhar PH (1992) A brief history of research on phantom alternatives: evidence for seven empirical generalizations about phantoms. Basic Appl Soc Psychol 13(1):103–122
Rothkirch I, Granert O, Knutzen A, Wolff S, Gövert F, Pedersen A, Zeuner KE, Witt K (2018) Dynamic causal modeling revealed dysfunctional effective connectivity in both, the cortico-basal-ganglia and the cerebello-cortical motor network in writers' cramp. Neuroimage Clinical 18:149–159
Stephan KE, Penny WD, Daunizeau J, Moran RJ, Friston KJ (2009) Bayesian model selection for group studies. Neuroimage 46(4):1004–1017
Swick D, Ashley V, Turken U (2011) Are the neural correlates of stopping and not going identical? Quantitative meta-analysis of two response inhibition tasks. Neuroimage 56(3):1655–1665
Trueblood JS (2012) Multialternative context effects obtained using an inference task. Psychon Bull Rev 19(5):962–968
Trueblood JS, Brown SD, Heathcote A, Busemeyer JR (2013) Not just for consumers: context effects are fundamental to decision making. Psychol Sci 24(6):901–908
Trueblood JS, Pettibone JC (2017) The phantom decoy effect in perceptual decision making. J Behav Decis Mak 30(2):157–167
Tsetsos K, Chater N, Usher M (2012) Salience driven value integration explains decision biases and preference reversal. Proc Natl Acad Sci 109(24):9659–9664
Turner BM, Forstmann BU, Love BC, Palmeri TJ, Van Maanen L (2017) Approaches to analysis in model-based cognitive neuroscience. J Math Psychol 76:65–79
Tzourio-Mazoyer N, Landeau B, Papathanassiou D, Crivello F, Etard O, Delcroix N, Mazoyer B, Joliot M (2002) Automated anatomical labeling of activations in SPM using a macroscopic anatomical parcellation of the MNI MRI single-subject brain. Neuroimage 15(1):273–289
Woo CW, Koban L, Kross E, Lindquist MA, Banich MT, Ruzic L, Andrews-Hanna JR, Wager TD (2014) Separate neural representations for physical pain and social rejection. Nat Commun 5:5380. https://doi.org/10.1038/ncomms6380
Yaple ZA, Yu R (2019) Fractionating adaptive learning: A meta-analysis of the reversal learning paradigm. Neurosci Biobehav Rev 102:85–94. https://doi.org/10.1016/j.neubiorev.2019.04.006
Yu R, Zhou X (2009) To bet or not to bet? The error negativity or error-related negativity associated with risk-taking choices. J Cogn Neurosci 21(4):684–696. https://doi.org/10.1162/jocn.2009.21034